International Journal of Heat and Technology
Vol. 43, No. 5, October, 2025, pp. 1909-1919
Journal homepage: http://iieta.org/journals/ijht

The Impact of Using Biogas, Biodiesel in the Combustion, Performance, and Emissions Parameters of Dual Fuel Diesel Engine

Duraid F. Maki[1*], Mohamed F. Al-Dawody[2], Khaled A. Al-Farhany[2], Naseer H. Hamza[2]

[1] Department of Mechanical Engineering, University of Babylon, Hilla 51002, Iraq
[2] Department of Mechanical Engineering, University of Al-Qadisiyah, Al-Qadisiyah 58002, Iraq

Corresponding Author Email: eng.duraid.f@uobabylon.edu.iq

https://doi.org/10.18280/ijht.430530

Received: 21 July 2025
Revised: 16 October 2025
Accepted: 24 October 2025
Available online: 31 October 2025

Keywords:
hybrid fuel, diesel-RK, biogas, spirulina green biodiesel, dual fuel engine

ABSTRACT

The present work deals with the thermal characteristics of a single cylinder 4-stroke diesel engine powered by regular diesel, 20% biodiesel derived from green spirulina algae, and 20% biogas, which are examined numerically using Diesel-RK software. The multi-zone combustion model is used, which treats each zone as an open thermodynamic system. In addition to neat diesel, the biodiesel is blended with conventional diesel and supplied to the engine. Another fuel is the 20% biogas is used as a dual fuel. As gas fuel 20% based on an energy basis. A combination of diesel, biodiesel, and biogas is called hybrid fuel. The outcomes revealed that peak pressures and heat release rates were decreased. Sauter mean diameter reduces by 16.2% and 15% for 20% biogas and hybrid forms, respectively. There is a slight reduction in brake thermal efficiency for all tested fuels. Using 20% biodiesel reported a lower increase in brake-specific fuel consumption by 3.1% compared to 8.3% and 5.3% in the case of 20% biogas and hybrid mode, respectively. The operation with 20% biogas, 20% biodiesel, and hybrid forms reduces NO_X by 27.9%, 16.6%, and 8.45%, respectively. It can be observed that the utilized of 20% biogas or 20% biodiesel separately is preferable to use rather than combining them in hybrid mode. Other researchers' findings validate the results.

1. INTRODUCTION

The rapid growth of the global population is significantly increasing the demand for energy. The vast majority of energy consumed today comes from fossil fuels such as coal and gasoline [1]. Scientists predict that the world will face shortages of oil, gas, and coal resources in the near future [2]. It has been noted that internal combustion engines produce the most harmful pollution among mechanical engines. Reducing emissions from traditional fossil fuels one of the biggest threats to the planet remains a serious challenge for fuel suppliers and automobile manufacturers [3-6]. Because stricter limits on impurities are being adopted globally, research on clean fuels has become a crucial area of environmental study [7, 8]. The critical literature showed that adding 20% biodiesel to diesel fuel can reduce CO and HC emissions but slightly increase NOx emissions. On the other hand, the biogas is also an active biofuel that shows a promising potential for improving engine operation and stability under different conditions [9, 10]. Biogas is suitable for use in both internal combustion engines because it produces fewer emissions than liquid fossil fuels [11]. Many studies have investigated biogas in dual-fuel diesel engines. These studies focus on particular aspects, mainly engine performance, combustion characteristics, and emissions rates [12-15]. Yoon and Lee [16] practically investigated combustion patterns and diagrams. Their results were similar regarding combustion parameters but showed clear differences in soot and emission ratios. Qian et al. [17] reached similar results patterns and conclusions. The use of biogas combined with H_2 at different ratios in a direct-injection, air-cooled, four-stroke single-cylinder engine was developed by Bouguessa et al. [18]. Hydrogen had a supportive effect on reducing NOX emissions and unburned residues in the exhaust. Tests were conducted on a turbocharged, direct-injection diesel engine using diesel as a pilot fuel and biogas enriched with various amounts of hydrogen. However, hydrogen addition can increase cylinder pressure at the same load and provide more powerful performance, according to many researchers [18, 19]. Deheri et al. [20] tested the use of dual-fuel mode and its effect on engine performance and emissions. Nanoparticles were added in small fractions to biodiesel to increase thermal efficiency and brake power. In the study by Karthik et al. [21], biogas–DME was reported to reduce soot formation in diesel engines. Furthermore, the study examined the increase in NOX content when DME was dominant. In order to identify the combustion by-products (exhaust emissions) and their characteristics from both light- and heavy-duty diesel cars, Ga and Thai [22] and Singh et al. [23] conducted research utilizing a portable emission tester (PET) in the city of Imphal, India, across twelve commercial locations. Throughout the trial, the outside temperature fluctuated between 23.5 and 28°C, and the relative humidity was 65 ± 15%. Gürbüz et al. [24] used an ethanol–diesel blend

(ED%) in a dual-fuel diesel engine at different load and speed conditions. Compared to reference diesel and ED95 single-fuel settings, NOX decreased by around 47–67% at all engine speeds during the dual-fuel experimental investigations, while smoke opacity remained constant. An overview of earlier research indicates that a large number of publications using biodiesel have been published. Meanwhile, few studies have examined the use of single and dual-fuel modes as well as hybrid fuels that include various combinations of other fuel sources, such as biodiesel and biogas. This gap can be closed by employing Diesel-RK software to quantitatively investigate and analyze combustion, performance, and emissions characteristics. The present study examines a variety of fuel blends as the initial baseline for comparison, starting with pure diesel without any additions. In the dual fuel mode, part of the DF is replaced by energy of 20% biogas that contains (55% CH4, 35% CO_2, 10% H_2O). After that, the engine is supplied with energy substitution of 30% DME rather than biogas. The thermal response of the engine for the operation of biogas and DME is checked against the original baseline case (DF).

2. MATERIALS AND METHOD

Table 1. Properties of research's fuels

Properties	Iraq Diesel Fuel (DF)	20% Biogas	30% DME
C%	0.87	0.78	0.77
H%	0.13	0.12	0.13
O%	0.004	0.102	0.106
Molecular mass (kg/kmol)	190	157.21	146.80
Density (kg/m^3)	830	664.23	766.48
Surface tension (N/m)	0.028	0.023	0.022
Viscosity (Pa.s)	0.0023	0.0018	0.0016
Heating value (MJ/kg)	45.83	36.67	40.61
Cetane number	53.40	42.72	55.38

Table 2. Motor specifications used in experimental tests

Engine Parameter	Descrption
Engine Make	Kirloskar diesel engine
Engine type	4-stroke, single-cylinder
Bore × Stroke	87.5 mm × 110 mm
Swept volume	0.553 m^3
Clearance volume	0.03687 m^3
Compression ratio	17.5
Rated output	3.7 kW @ 1500 rpm
Injection pressure	160 bar
Injection timing	20º BTDC
Discharge Coefficient	0.65
Nozzle Diameter	0.15 mm

The present study examines a variety of fuel blends as the initial baseline for comparison, starting with neat diesel (mono fuel) with no additions. The biogas utilized in this work contains (55% CH_4, 35% CO_2, and 10% H_2O), which is used separately in dual fuel mode for 20% (energy replacement). The green algae (spirulina) are used to produce green biodiesel via a transesterification process. The production process is thoroughly described in the previous studies [24-27]. It is blended with diesel at a ratio of 20% by volume. Different studies on biodiesel production from microalgae biomass are listed in Ebhodaghe et al. [6]. The hybrid fuel combines all the mentioned fuels in their percentages and is referred to as (60% Diesel+20% Biogas+20% Biodiesel). Table 1 lists the chemical and physical properties of Iraqi diesel, biogas, and DME. Those results were obtained by tests in Aldoora refinery, Baghdad, Iraq. For numerical simulation, Table 2 shows the engine's technical specifications.

3. NUMERICAL ANALYSIS

3.1 Conservation equations

The mass conservation equation in an open system is:

$$\frac{dm}{dt} = \sum_i m_i \quad (1)$$

m_i: represents each mass of species flow rate
t: the time
i: indicates the species number
The species conservation mathematical equation is given by Eq. (2).

$$Y_i = \sum_i \frac{m_i}{m} \quad (2)$$

where, Y_i, is pointed to specie mass fraction.
In open thermodynamic systems, standard energy equation can write as:

$$\frac{d(mu)}{dt} = -p\frac{dv}{dt} + \frac{dQ_{ht}}{dt} + \sum_i m_i h_i \quad (3)$$

Eq. (3) is the total system energy change time rate.
u: specific internal energy
m: specie mass
p: pressure
v: specific volume
Q_h: amount of system heat
H: enthalpy of specie

3.2 The simulation software

In this study, the Russian thermodynamic software Diesel-RK is used. This model is based on a multi-zone combustion process. Zones are treated as open thermodynamic systems. This software has an optimization tool that uses the four-stroke and two-stroke internal combustion engine to optimize and assess using the DIESEL-RK simulation tool.

3.2.1 The spray evaluation modelling
The model of multi zones fuel spray is implemented in this study [28]. Various zones separate the fuel spray injected into the combustion chamber of the engine [29].
The (EFM), which is an abbreviation of (elementary fuel mass), is the mass of fuel moving from the fuel injector to a spray tip. Eq. (4) gives the mathematical equation of this movement.

$$\left(\frac{V}{V_O}\right)^{\frac{3}{2}} = 1 - \frac{l}{lm} \quad (4)$$

V: represents the measure of the EFM's current speed,
V_O: initial speed of EFM at nozzle injector,
l: The space between the elementary fuel mass and the nozzle injector. The elementary fuel mass is penetrated for

time even before a spray reaches its termination. A simplified spray scheme is shown in Figure 1 to solve Eq. (4) as:

$$3l_m[1-[1-\frac{l}{l_m}]^{0.333}]-V_0\tau_K=0 \quad (5)$$

where, τ_k: - For the EFM, the travel period equals the distance from an injector nozzle. When the EFM of a spray tip ceases operation, then $l=l_m$ and $\tau_k=\tau_m$.
where, τ_m is a travel period for the EFM to reach the spray's front before ending.

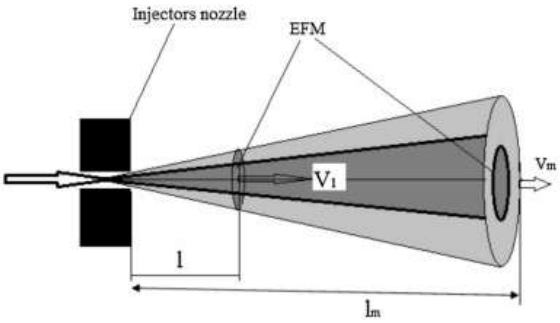

Figure 1. A spray nozzle diagram [27]

The rewriting of formula (5) yield:

$$l_m=V_o\frac{\tau_m}{3} \quad (6)$$

In order to determine the speed and length of EFM, Eqs. (3) to (6) are used:

$$V=V_o\left(1-\frac{\tau_k}{\tau_m}\right)^2 \quad (7)$$

$$l=[1-(1-\frac{\tau_k}{\tau_m})^3]l_m \quad (8)$$

3.2 Allocation of fuel to the spray

Seven different zones are the result of spray division, as shown in Figure 2.

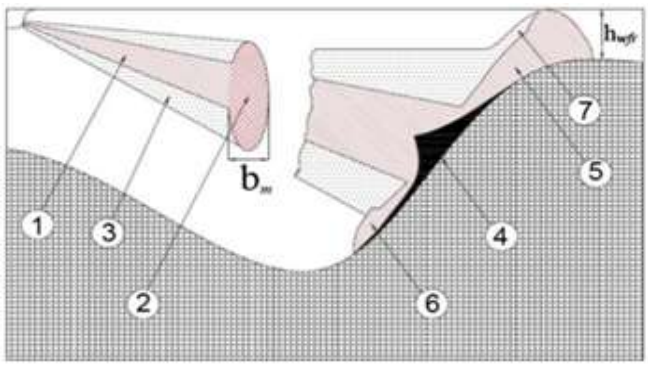

Figure 2. Zones of spray fuel [30]

It's notable that the burning and evaporation of each zone have their specific requirements.

Three zones must be considered during the free spray time prior to jet impingement. The subsequent enumeration is:

1. intensive forward front.
2. thick conical core.
3. The dilution process happens in outer shell.

The flow variation properties near the wall make the calculation of evaporated fuel complex. Therefore, its primary goal is to recognize between parameters for transfer of heat, simulate the regions, and fuel mass at the flow boundary by free spray calculations. A new set of locations needs to be evaluated after contact with the wall.

4. Highly dense near wall flow (NWF) on the surface of the piston.
5. Dense center of the NWF cone.
6. A dilution in external region of the NWF.
7. Densely populated in forward of NWF.

3.3 Model of heat release

The combustion process consists of four-stages, each having distinct physical and chemical features. A representation of the phases can be estimated below [29]:

Ignition delay period phase.
calculation the self-ignition delay by:

$$\tau=3.8/10^6*\sqrt{\frac{T}{P}}*e^{\left(\frac{Ea}{8.312T}-\frac{70}{CN+25}\right)}*(n*1-1.6/10^4) \quad (9)$$

The premixed combustion phase (combustion resulting from air /vapor of fuel being blended) as:

$$\frac{dx}{dt}=\varphi_1\left\{\frac{d\sigma_u}{d\tau}\right\}+\varphi_0*\left\{A_0*(0.1\sigma_{ud}+x_0)(\sigma_{ud}-x_0)\left(\frac{m_f}{V_i}\right)\right\} \quad (10)$$

Diffusive combustion phase (injected fuel combustion).
The following is a definition of the heat release rate:

$$\frac{dx}{d\tau}=\left\{(\emptyset-x)(\sigma_u-x)*\left\{\frac{m_f}{V_c}\right\}*A_2\right\}*\varphi_2+\left\{\frac{d\sigma_u}{d\tau}\right\}*\varphi_1 \quad (11)$$

Phase of late burning (fuel burning after injection).
Following is a formula for calculating the rate of heat release:

$$\frac{dx}{d\tau}=(\epsilon_b\emptyset-x)(1-x)*A_3*\varphi_3*K_T \quad (12)$$

$\varphi_0=\varphi_3=\varphi_2=\varphi_1$, these functions describe fuel vapor's total combustion in each zone.

3.4 A model for predicting NO_X and smoke formation

The Zel'Dovich extended mechanism is adopted by Diesel-RK program. This mechanism is used to describe the nitrogen oxides composition of diesel engine. NO_X emissions are presented the NO_2 and NO. Zel'Dovich's mechanism has been selected:

$$O_2\leftrightarrow 2O \quad (13)$$

$$O+N_2\leftrightarrow NO+N \quad (14)$$

$$O_2+N\leftrightarrow NO+O \quad (15)$$

The concentration of oxygen, as given in Eq. (15), has an effect on the rate of this reaction. The Eq. (16) is used to estimate the nitrogen oxide volume concentration [29]:

$$\frac{d[NO]}{d\theta} = \frac{2.33*10^7*P\{1-\left(\frac{[NO]}{[NO]_e}\right)^2\}*[N_2]_e[O]_e*e^{\frac{-38020}{T_z}}}{RT_z\left[1+\frac{[NO]}{[O_2]_e}*\left(\frac{2365}{T_z}\right)e^{\frac{3365}{T_z}}\right]}\left[\frac{1}{rps}\right] \quad (16)$$

Eq. (17) to calculate the soot concentration in relation to natural conditions:

$$[C] = \int_{\theta_B}^{480} \frac{d[C]}{d\tau} * \frac{d\theta}{6n} * \left[\frac{0.1}{P}\right]^{\gamma} \quad (17)$$

The Bosch smoke number is used to measure emitted particulate matter as in equation below:

$$[PM] = \left[\ln\frac{10}{10-Bosch}\right]^{1.206} * 565 \quad (18)$$

The combining of NO_X and PM emissions is given by Eq. (19) which is developed by Kuleshov [29] and known as the SE:

$$SE = C_{NO}\left[\frac{NO_X}{7}\right] + C_{PM}\left[\frac{PM}{0.15}\right] \quad (19)$$

4. CODE VALIDITY

Numerous studies discuss the simulation, practical tests in such types of fuels and engines [30-33]. Under the same operating conditions, full load at 1500 rpm and a compression ratio of 17.5:1, the current findings are compared with three distinct studies conducted by Rajak and Verma [34], Dasari et al. [35], and Prakash et al. [36], which were selected for validation. Rajak and Verma [34] performed a numerical investigation on the impact of various biofuels on diesel engine performance, while Dasari et al. [35] and Prakash et al. [36] experimentally examined the effects of using castor methyl ester (bioethanol and CME) on diesel engine parameters. Table 3 provides a technical summary of the engines used for validation. Common diesel fuel is considered for powering the engines in all cases, as it is consistent across the literature, and the same approach applied to diesel is extended to other fuel mixtures. Figure 3 illustrates the progression of spray penetration at full load for diesel. Injection starts at 20° before top dead center (BTDC). In this study, the maximum penetration of 84.91 mm was recorded at a crank angle of 372°, compared with 81.9 mm reported by Rajak and Verma [34], while the lowest penetration of 73.4 mm was at the same crank angle [35, 36]. Injection pressure plays an important role in determining spray penetration, and the current study exhibits comparable behavior with acceptable variance. Figure 4 shows the development of diesel cylinder pressure over 140° of crank angle, spanning from 60° BTDC to 80° ATDC, as this range exhibits the most significant changes in pressure history. The peak pressure is observed between 3° and 5° ATDC in all examined models, with values ranging from 95.5 bar to 100 bar. The comparison shows strong convergence with only slight differences; a small discrepancy of approximately 4% is noted. Further validation of the obtained results was performed by comparing with the studies of Barik and Sivalingam [37] and Feroskhan et al. [38]. Engine dimensions, test conditions, and fuel properties were incorporated into the software database library. For volumetric efficiency (shown in Figure 5), the deviation is around 1.7% in the case of Barik and Sivalingam [37] and 1.13% in the case of Feroskhan et al. [38] compared with the results of the present work. The low deviation percentages demonstrate that Diesel-RK is a reliable tool for simulating the combustion process in internal combustion engines.

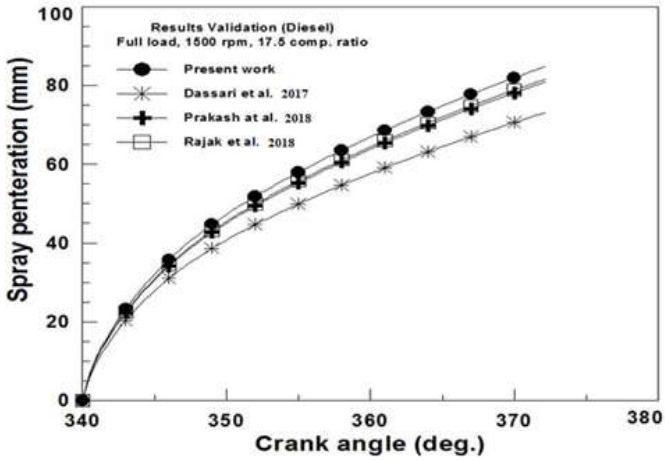

Figure 3. Validation of spray diffusion versus crank angle

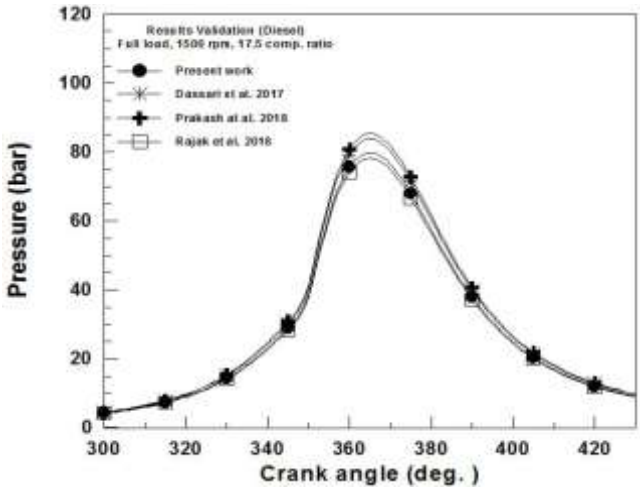

Figure 4. Validation of cylinder pressure versus crank angle

Table 3. Specifications of three engine setups used for validation

Test Facility	Kirloskar as Setup 1	Kiroskar TV1 as Setup 2	Legion Brothers as Setup 3
Engine type	CI, 1 cylinder, 4 stroke	CI, 1 cylinder, 4 stroke	CI, 1 cylinder, 4 stroke
bore× stroke	87.5 × 110 mm	87.5 × 110 mm	80 × 110 mm
Cooling system	air	air	water
Comp. ratio	17.5: 1	17.5: 1	17.5: 1
Rated ou power@ 1500	5.22 kW	5.2 kW	3.7 kW
Inject. Pressure	200 bar	160 bar	200 bar
Inject. timing	23° BTDC	20° BTDC	23° BTDC

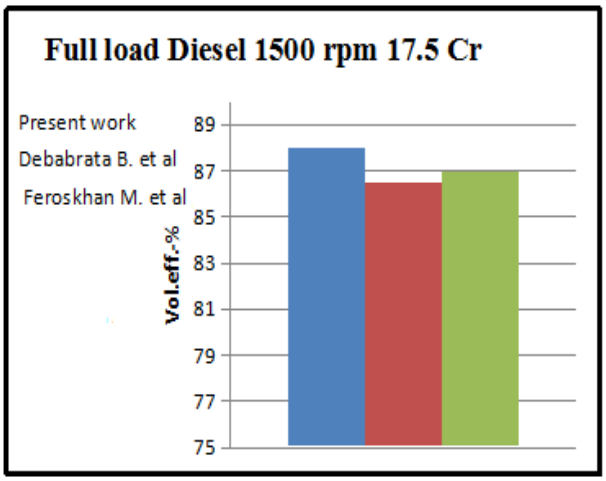

Figure 5. Validation of the model's volumetric efficiency

5. RESULTS AND DISCUSSION

5.1 Combustion study

Engine cylinder pressure is the pressure generated inside a diesel engine during its four strokes. It indicates the efficiency of air–fuel mixing and the quality of combustion [25]. Cylinder pressure strongly influences both the engine's power output and the emission characteristics of the fuel. Figure 6 presents the variation of cylinder pressure with crank angle at 100% load for the tested fuels at corresponding cylinder pressures and heat release rates. The interval between 40° BTDC and 40° ATDC shows the most clear differences, facilitating a direct comparison among the fuels under investigation.

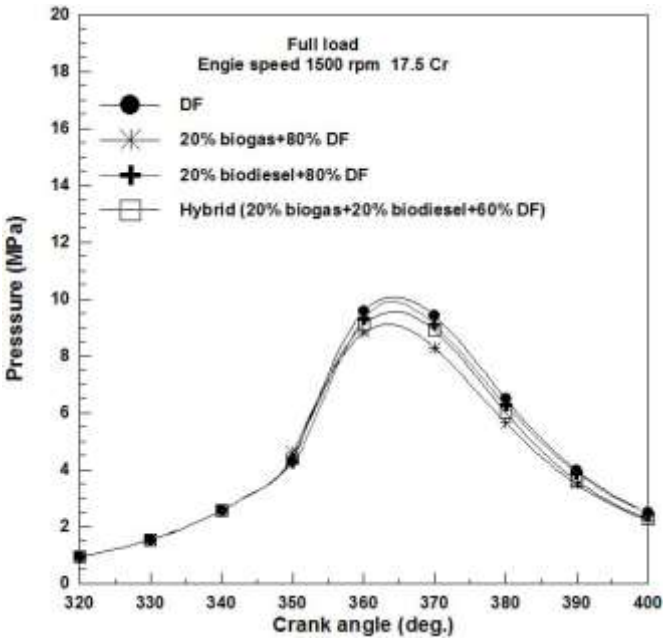

Figure 6. Pressure development per crank angle

In the initial phase of combustion, the rate of heat release governs the peak cylinder pressure. This phenomenon mainly arises from the intake of fuel components that release heat uncontrollably [39]. All fuels show smooth and uniform pressure profiles. For pure diesel, the peak pressure reaches 10.07 MPa. For a blend of diesel with 20% biodiesel, the peak decreases to 9.89 MPa, while dual-fuel operation with 20% biogas yields a lower peak of 9.10 MPa. Hybrid fuel records a peak pressure of 9.54 MPa. Generally, single or hybrid fuel blends result in lower cylinder pressures compared with net diesel, mainly due to their lower heating values. Specifically, 20% biogas reduces pressure by 9.6%, while 20% biodiesel and hybrid fuel reduce it by 1.73% and 5.17%, respectively. These findings align with Barik and Sivalingam [37].

The heat release profiles at full load are shown in Figure 7. Combustion behavior is governed by the air/fuel mixing rate and the calorific value of the fuel. Dual-fuel operation presents a more complex combustion process than single-fuel operation because both liquid and gaseous phases combust simultaneously. In such systems, the heat release rate (HRR) depends strongly on the quality of the intake charge blend [17]. Compared with net diesel, all fuel blends—whether used separately or in hybrid form—exhibit lower heat release due to lower calorific values. Combustion begins earlier, and ignition delay shortens with 20% biodiesel or 20% biogas. The maximum HRR for diesel is 69 J/deg, compared with 56, 67.5, and 61.5 J/deg for biogas, biodiesel, and hybrid fuels, respectively.

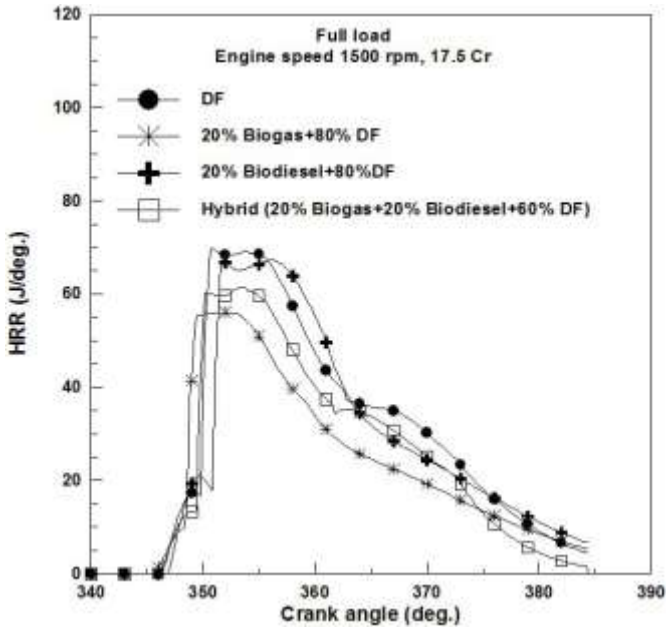

Figure 7. Heat release profile per crank angle

Measuring combustion temperature inside the combustion chamber is technically challenging and often requires specialized equipment. For example, studies modified a fast-response thermocouple to measure instantaneous gas temperature [40-42]. Figure 8 shows the mean zonal combustion temperatures. Diesel yields the highest temperatures due to its higher energy release. The maximum average temperatures for 20% biodiesel, 20% biogas, and hybrid fuel are 2740 K, 2840 K, and 2800 K, respectively. Because combustion temperature drives NOx formation, decreases in temperature directly reduce NOx emissions.

Figure 9 presents the effect of different fuel blends on free-spray tip penetration length, starting at 20° BTDC and ending at 13° ATDC. Several factors influence spray dynamics, including in-cylinder pressure, injection pressure and timing, air density, viscosity, surface tension, and nozzle diameter, with injection pressure having the strongest effect [12]. Hybrid

fuel shows the longest penetration length, followed by biogas, biodiesel, and diesel. For 20% biodiesel, 20% biogas, and hybrid fuel, penetration increases by 1.56%, 4.2%, and 6.1%, respectively. Differences in surface tension, density, and viscosity distinguish biogas and biodiesel from diesel and affect atomization and spray behavior.

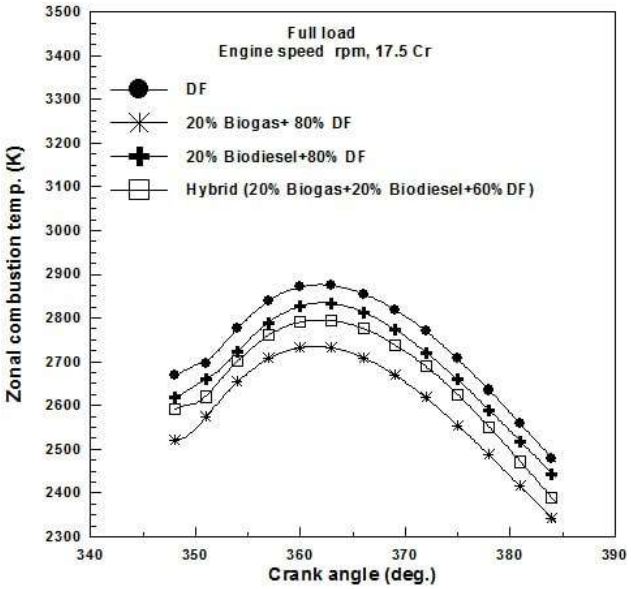

Figure 8. Zonal temperature distribution per crank angle

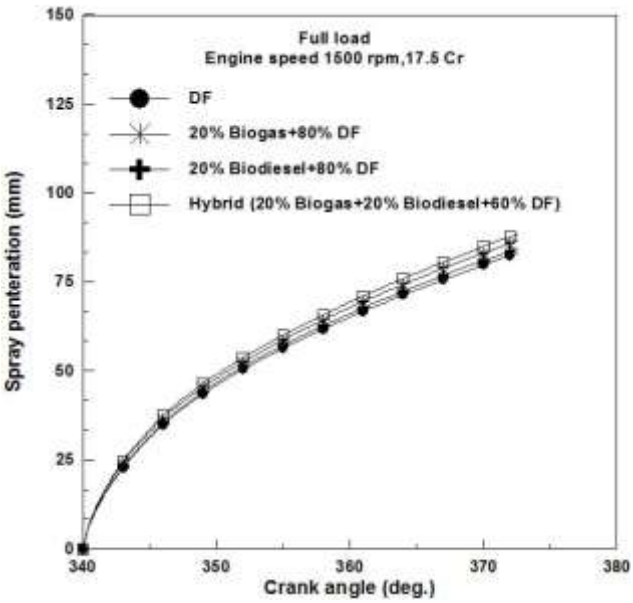

Figure 9. Free spray penetration per crank angle

Biodiesel typically has higher surface tension and viscosity, causing larger droplets and a higher Sauter Mean Diameter (SMD). By altering fuel properties, adding biogas or biodiesel influences combustion characteristics, engine performance, emissions, thermal efficiency, and ultimately SMD. As shown in Figure 10, SMD is presented as a bar chart for the tested fuels. SMD increases as saturated FAME content increases. Due to its higher viscosity and surface tension, biodiesel increases SMD by 1.45%. Larger droplets burn more slowly and at lower velocities. Replacing 20% biodiesel with 20% biogas reduces SMD by 16.18% due to lower viscosity. Combining biogas, biodiesel, and diesel reduces SMD by about 15%.

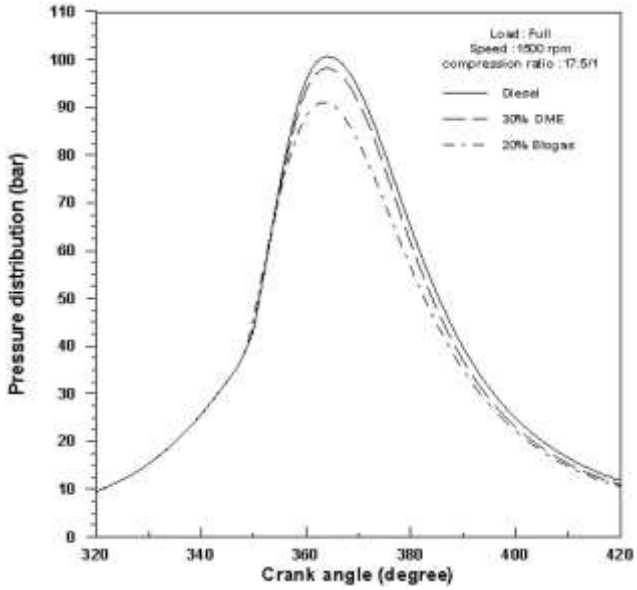

Figure 10. The comparison between baseline DF, 30% DME, and 20% biogas pressure distribution

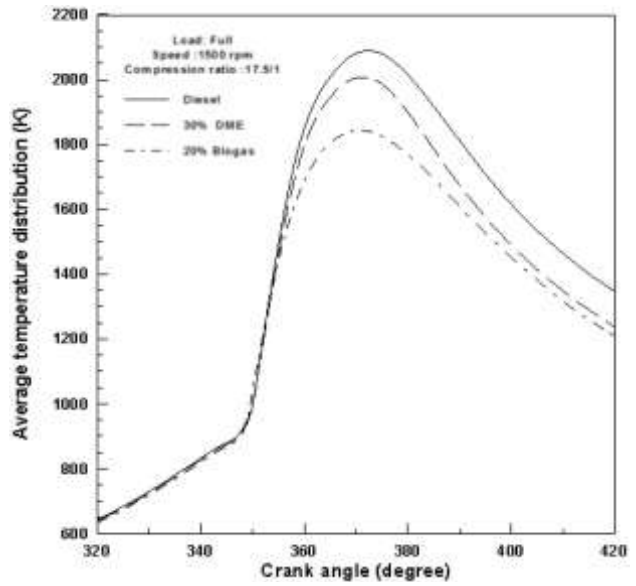

Figure 11. Average temp. distribution comparison for diesel, 30% DME, and 20% biogas

Ignition delay (ID) consists of physical delay and chemical delay. The physical delay is the time needed for fuel injection, atomization, vaporization, and mixing. Factors such as boiling point, latent heat, injection pressure, and chamber temperature affect it [43]. The chemical delay is the time needed for pre-combustion chemical reactions. It is governed by reaction kinetics, temperature, pressure, and fuel composition [44-47].

Figure 10 also shows combustion pressure development over a 100° crank-angle interval (320°–420°), where major changes occur. Diesel, biogas, and dimethyl ether (DME) follow similar trends with differences only in peak pressure. Diesel reaches 100.7 bar, while 20% biogas and 30% DME reduce pressure by 2.45% and 9.6%, respectively, due to their lower heating values.

Figure 11 shows the variation in average combustion temperature. The lowest temperature is observed for 20% biogas, and the highest for diesel. Lower combustion temperatures produce lower flame temperatures and thus

reduce NOx emissions. Differences in density, viscosity, and heating value contribute to this behavior. Using 30% DME with diesel reduces peak temperature by 3.9%, whereas 20% biogas reduces it by 11.75%.

Figures 12 and 13 display ignition delay as a function of fuel type. ID is defined as the time between the start of injection and the start of combustion. Engine characteristics such as cetane number, injection pressure, compression ratio, and intake temperature strongly influence ID. A higher cetane number means shorter ID and better ignition quality. Diesel has an ID of 9.37°, while biogas, biodiesel, and hybrid fuel have IDs of 8.06°, 8.93°, and 9.00°, respectively.

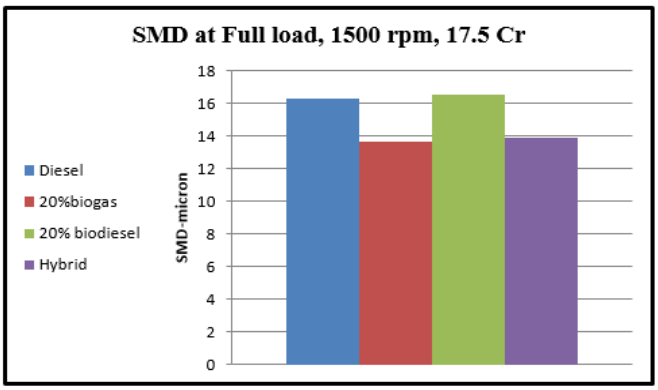

Figure 12. SMD values for different fuel blends

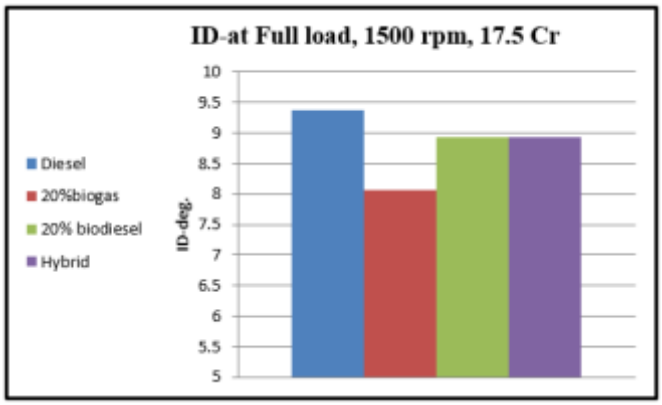

Figure 13. ID values for different fuel blends

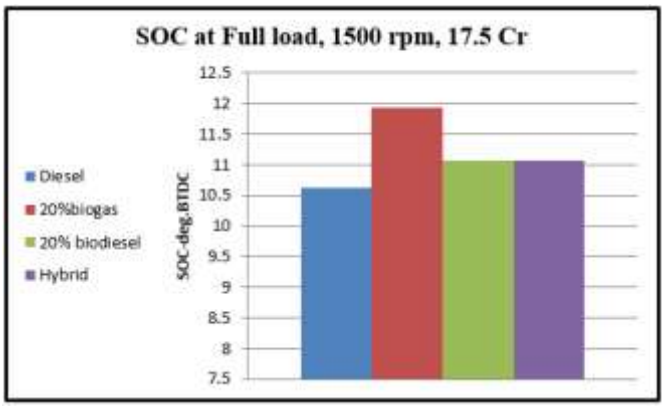

Figure 14. SOC values for different fuel blends

High temperatures can cause thermal cracking in biodiesel, forming lighter compounds that ignite sooner, decreasing ID. Figure 14 highlights the start of combustion (SOC). Longer ID leads to later SOC. For diesel, SOC occurs at 10.62° BTDC, while for biogas and hybrid fuels, SOC occurs at 11.93° and 11.07° BTDC, respectively. The ID for biodiesel is nearly identical to hybrid fuel. These results agree with Murad and Al-Dawody [25].

5.2 Performance study

Brake Thermal Efficiency (BTE) and Brake Specific Fuel Consumption (BSFC) are considered the primary performance parameters. Figure 15 presents BTE values for all engine loads. BTE decreases when biogas, biodiesel, or their combination is used. Due to tested differences in heating values, the use of 20% biogas reduces BTE by 4% compared with reductions of 1.3% and 0.87% for hybrid fuel and biodiesel, respectively. Figure 16 shows the BSFC values for the selected fuels. To produce the same power output, more fuel is required as density and viscosity increase, which significantly impacts BSFC. The use of biodiesel and biogas/diesel blends increases BSFC because the heating values of methyl esters are approximately 12.4% lower than those of pure diesel. Similar trends were reported by Barik and Sivalingam [37]. Biogas consumes 8.35% more fuel than conventional diesel, while the BSFC of the engine increases by 3.1% and 5.2% when powered by biodiesel and the biodiesel/biogas blend, respectively. These findings indicate that operating an engine with biodiesel or biogas individually is preferable to combining them into a hybrid fuel.

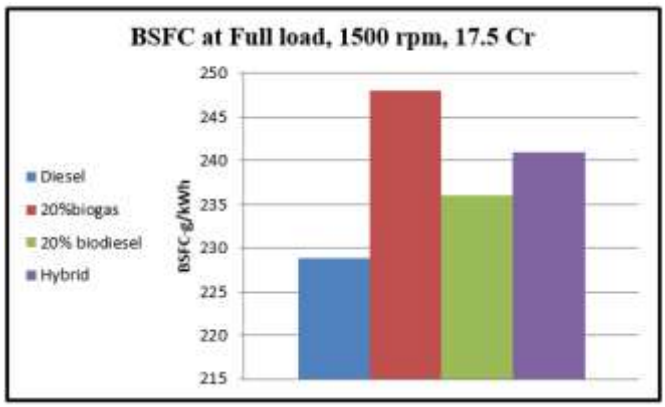

Figure 15. BSFC values for different fuel blends

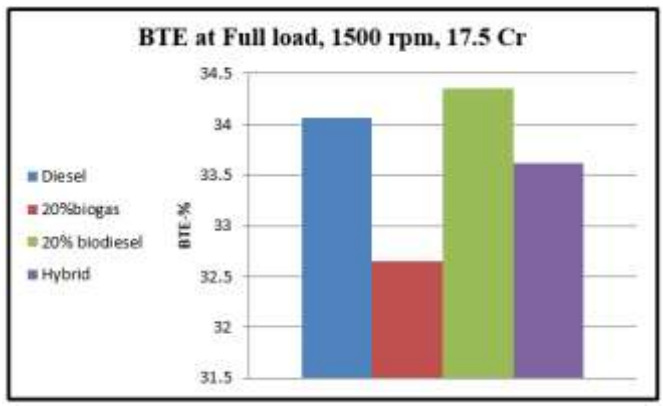

Figure 16. BTE values for different fuel blends

5.3 Emission study

To compare pollutant emissions, full-load conditions

representing the lowest air–fuel ratio are considered, as this point makes differences between fuels more apparent. Figure 17 shows the NOx emissions for the tested fuels. The formation of NOx is promoted by three parameters: Rising temperatures (which provide the energy needed to react), an oxygen rich environment (which supplies the required reactants), and sufficient time (this sufficient time allows the reaction to reach the end completely). Those parameters help to reduce NOx emissions [48, 49].

It can be noted that NOx emissions are highest for diesel, while biogas, biodiesel, and the biogas/biodiesel hybrid produce lower NOx emissions by 27.9%, 16.54%, and 8.5%, respectively. Reduced combustion temperatures and oxygen content are primarily responsible for this reduction, directly decreasing NOx formation. Similar findings were reported by Rajak et al. [31]. To avoid the trade-off between particulate matter (PM) and NOx emissions, one emission parameter often increases as another decreases. Based on the obtained results, there is a clear trade-off between NOx and PM emissions. This is primarily attributed to oxygen content, which can simultaneously reduce carbon (PM) emissions while increasing NOx formation, or vice versa. Researchers have been working to reduce both PM and NOx emissions through multi-parametric optimization. The summary equation relating PM and NOx is denoted as the SE equation (Eq. (19)), which serves as the goal optimization function. Figure 18 shows the SE values for the fuels under consideration. Using 20% biogas with diesel reduces SE emissions by 5.4%, while 20% biodiesel and hybrid fuel reduce SE emissions by 33.26% and 5.62%, respectively. A decrease in SE values indicates that the increase in PM is smaller than the decrease in NOx, and vice versa.

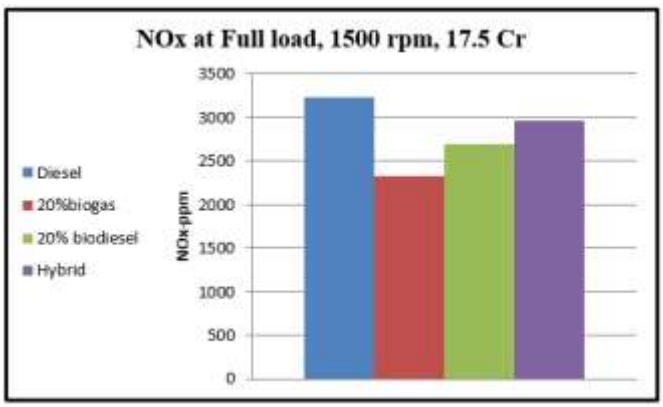

Figure 17. NO_X values for different fuel blends

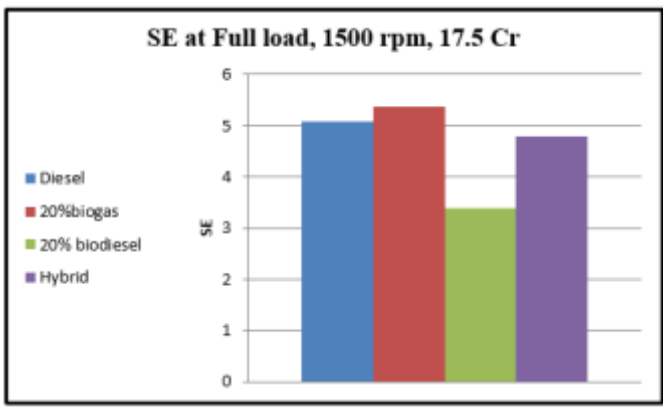

Figure 18. SE values for different fuel blends

6. CONCLUSIONS

The following conclusions are addressed:

1. All fuel results showed a minor reduction in-cylinder pressure, combustion zone temperature, and heat release rate.
2. The combustion of biogas and biodiesel begins earlier as a result of the shorter delay period as compared with standard diesel.
3. The SMD is lowered by 16.18% when 20% biogas is substituted for 20% biodiesel. SMD may be reduced by 15% by mixing diesel (hybrid fuel), biogas, and biodiesel. This has happened due to the decrease in viscosity.
4. Higher BSFC is observed for biogas and biodiesel when used separately or combined to gather.
5. The BTE is reduced slightly by 0.87% with the operation of 20% biodiesel, while the use of 20% biogas and hybrid mode reports a reduction of 4.12% and 1.3%, respectively.
6. The use of biogas or biodiesel alone caused a reduction in NOX by 27.89% and 16.54%, respectively. In meanwhile, the hybrid mode (doing together) resulted 8.44% reduction in NOX.
7. In terms of the summary emission, the 20% biodiesel beat biogas and hybrid mode. Because emissions are notably decreased by 33.26% when 20% biodiesel is used as fuel alone, they are increased by 5.40% and 5.62% when using 20% biogas or hybrid mode, respectively.
8. It might be concluded from the overall findings from this study that using 20% biodiesel or 20% biogas separately is preferable to using both simultaneously.

An experimental investigation is recommended under different conditions, such as compression ratio, load, and engine speed, to validate the numerical results. As well as, feasibility study of using renewable fuel as a substitute for net diesel.

ACKNOWLEDGMENTS

The authors are thankful to the Deanship of Graduate Studies and Scientific Research at the University of Bisha for supporting this work through the Fast-Track Research Support Program.

REFERENCES

[1] Gupta, P., Rajak, U., Verma, T.N., Arya, M., Singh, T.S. (2023). Impact of fuel injection pressure on the common rail direct fuel injection engine powered by microalgae, kapok oil, and soybean biodiesel blend. Industrial Crops and Products, 194: 116332. https://doi.org/10.1016/j.indcrop.2023.116332

[2] Soleimani khorramdashti, M., Giri, M.S., Majidian, N. (2022). Design and optimization of lipids extraction process based on supercritical CO_2 using Dunaliella Tertiolecta microalga for biodiesel production. Arabian Journal of Chemistry, 15(7): 103920. https://doi.org/10.1016/j.arabjc.2022.103920

[3] Kesharvani, S., Verma, T.N., Dwivedi, G. (2023). Computational analysis of chlorella protothecoides

biofuels on engine combustion, performance and emission. Sustainable Energy Technologies and Assessments, 55: 102972. https://doi.org/10.1016/j.seta.2022.102972
[4] Mohsen, M.J., Al-Dawody, M.F., Jamshed, W., El Din, S.M., Abdalla, N.S.E., Abd-Elmonem, A., Iqbal, A., Shah, H.H. (2023). Experimental and numerical study of using of LPG on characteristics of dual fuel diesel engine under variable compression ratio. Arabian Journal of Chemistry, 16(8): 104899. https://doi.org/10.1016/j.arabjc.2023.104899
[5] Mabrouki, J., Abbassi, M.A., Guedri, K., Omri, A., Jeguirim, M. (2015). Simulation of biofuel production via fast pyrolysis of palm oil residues. Fuel, 159: 819-827. https://doi.org/10.1016/j.fuel.2015.07.043
[6] Ebhodaghe, S.O., Imanah, O.E., Ndibe, H. (2022). Biofuels from microalgae biomass: A review of conversion processes and procedures. Arabian Journal of Chemistry, 15(2): 103591. https://doi.org/10.1016/j.arabjc.2021.103591
[7] Abid, U., Gill, Y.Q., Irfan, M.S., Umer, R., Saeed, F. (2021). Potential applications of polycarbohydrates, lignin, proteins, polyacids, and other renewable materials for the formulation of green elastomers. International Journal of Biological Macromolecules, 181: 1-29. https://doi.org/10.1016/j.ijbiomac.2021.03.057
[8] Andrade Torres, F., Doustdar, O., Herreros, J.M., Li, R., Poku, R., Tsolakis, A., Martins, J., Vieira de Melo, S.A.B. (2021). A comparative study of biofuels and Fischer–Tropsch diesel blends on the engine combustion performance for reducing exhaust gaseous and particulate emissions. Energies, 14(6): 1538. https://doi.org/10.3390/en14061538
[9] Kalligeros, S., Zannikos, F., Stournas, S., Lois, E., Anastopoulos, G., Teas, C., Sakellaropoulos, F. (2003). An investigation of using biodiesel/marine diesel blends on the performance of a stationary diesel engine. Biomass and Bioenergy, 24(2): 141-149. https://doi.org/10.1016/S0961-9534(02)00092-2
[10] Al-Dawody, M.F., Bhatti, S.K. (2013). Optimization strategies to reduce the biodiesel NOx effect in diesel engine with experimental verification. Energy Conversion and Management, 68: 96-104. https://doi.org/10.1016/j.enconman.2012.12.025
[11] Shabir, S., Ilyas, N., Saeed, M., Bibi, F., Sayyed, R.Z., Almalki, W.H. (2023). Treatment technologies for olive mill wastewater with impacts on plants. Environmental Research, 216: 114399. https://doi.org/10.1016/j.envres.2022.114399
[12] Ahmed, S.A., Zhou, S., Zhu, Y., Tsegay, A.S., Feng, Y., Ahmad, N., Malik, A. (2020). Effects of pig manure and corn straw generated biogas and methane enriched biogas on performance and emission characteristics of dual fuel diesel engines. Energies, 13(4): 889. https://doi.org/10.3390/en13040889
[13] Ambarita, H. (2017). Performance and emission characteristics of a small diesel engine run in dual-fuel (diesel-biogas) mode. Case Studies in Thermal Engineering, 10: 179-191. https://doi.org/10.1016/j.csite.2017.06.003
[14] Barik, D., Murugan, S. (2016). Effects of diethyl ether (DEE) injection on combustion performance and emission characteristics of Karanja methyl ester (KME)–biogas fueled dual fuel diesel engine. Fuel, 164: 286-296. https://doi.org/10.1016/j.fuel.2015.09.094
[15] Mahla, S.K., Safieddin Ardebili, S.M., Sharma, H., Dhir, A., Goga, G., Solmaz, H. (2021). Determination and utilization of optimal diesel/n-butanol/biogas derivation for small utility dual fuel diesel engine. Fuel, 289: 119913. https://doi.org/10.1016/j.fuel.2020.119913
[16] Yoon, S.H., Lee, C.S. (2011). Experimental investigation on the combustion and exhaust emission characteristics of biogas–biodiesel dual-fuel combustion in a CI engine. Fuel Processing Technology, 92(5): 992-1000. https://doi.org/10.1016/j.fuproc.2010.12.021
[17] Qian, Y., Sun, S., Ju, D., Shan, X., Lu, X. (2017). Review of the state-of-the-art of biogas combustion mechanisms and applications in internal combustion engines. Renewable and Sustainable Energy Reviews, 69: 50-58. https://doi.org/10.1016/j.rser.2016.11.059
[18] Bouguessa, R., Tarabet, L., Loubar, K., Belmrabet, T., Tazerout, M. (2020). Experimental investigation on biogas enrichment with hydrogen for improving the combustion in diesel engine operating under dual fuel mode. International Journal of Hydrogen Energy, 45(15): 9052-9063. https://doi.org/10.1016/j.ijhydene.2020.01.003
[19] Khatri, N., Khatri, K.K. (2020). Hydrogen enrichment on diesel engine with biogas in dual fuel mode. International Journal of Hydrogen Energy, 45(11): 7128-7140. https://doi.org/10.1016/j.ijhydene.2019.12.167
[20] Deheri, C., Acharya, S.K., Thatoi, D.N., Mohanty, A.P. (2020). A review on performance of biogas and hydrogen on diesel engine in dual fuel mode. Fuel, 260: 116337. https://doi.org/10.1016/j.fuel.2019.116337
[21] Karthik, T., Banapurmath, N.R., Basavarajappa, D.N., Ganachari, S.V., Kulkarni, P.S., Harari, P.A. (2022). Effect of injection timing on the performance of dual fuel engine fueled with algae nano-biodiesel blends and biogas. Materials Today: Proceedings, 59: 289-296. https://doi.org/10.1016/j.matpr.2021.11.156
[22] Ga, B.V., Thai, P.Q. (2020). Soot emission reduction in a biogas-DME hybrid dual-fuel engine. Applied Sciences, 10(10): 3416. https://doi.org/10.3390/app10103416
[23] Singh, T.S., Rajak, U., Verma, T.N., Nashine, P., Mehboob, H., Manokar, A.M., Afzal, A. (2022). Exhaust emission characteristics study of light and heavy-duty diesel vehicles in India. Case Studies in Thermal Engineering, 29: 101709. https://doi.org/10.1016/j.csite.2021.101709
[24] Gürbüz, H., Demirtürk, S. (2020). Investigation of dual-fuel combustion by different port injection fuels (neat ethanol and E85) in a DE95 diesel/ethanol blend fueled compression ignition engine. Journal of Energy Resources Technology, 142(12): 122306. https://doi.org/10.1115/1.4047328
[25] Murad, M.E., Al-Dawody, M.F. (2020). Biodiesel production from spirulina microalgae oil. IOP Conference Series: Materials Science and Engineering, 928(2): 022127. https://doi.org/10.1088/1757-899X/928/2/022127
[26] Ryu, K., Zacharakis-Jutz, G.E., Kong, S.C. (2014). Performance enhancement of ammonia-fueled engine by using dissociation catalyst for hydrogen generation. International Journal of Hydrogen Energy, 39(5): 2390-2398. https://doi.org/10.1016/j.ijhydene.2013.11.098
[27] Al-Dawody, M.F., Jazie, A.A., Abbas, H.A. (2019). Experimental and simulation study for the effect of waste

cooking oil methyl ester blended with diesel fuel on the performance and emissions of diesel engine. Alexandria Engineering Journal, 58(1): 9-17. https://doi.org/10.1016/j.aej.2018.05.009
[28] Al-Dawody, M.F., Bhatti, S.K. (2014). Effect of variable compression ratio on the combustion, performance and emission parameters of a diesel engine fuelled with diesel and soybean biodiesel blending. World Applied Sciences Journal, 30(12): 1852-1858. https://doi.org/10.5829/idosi.wasj.2014.30.12.338
[29] Kuleshov, A.S. (2005). Model for predicting air-fuel mixing, combustion and emissions in di diesel engines over whole operating range. SAE Technical Papers. https://doi.org/10.4271/2005-01-2119
[30] Rajak, U., Nashine, P., Singh, T.S., Verma, T.N. (2018). Numerical investigation of performance, combustion and emission characteristics of various biofuels. Energy Conversion and Management, 156: 235-252. https://doi.org/10.1016/j.enconman.2017.11.017
[31] Al-Dawody, M.F., Rajak, U., Jazie, A.A., Al-Farhany, K., Saini, G., Verma, T.N., Nashine, P. (2022). Production and performance of biodiesel from Cladophora and Fucus green diesel. Sustainable Energy Technologies and Assessments, 53: 102761. https://doi.org/10.1016/j.seta.2022.102761
[32] Mohsen, M.J., Al-Dawody, M.F. (2022). The combustion characteristics of compression ignition engine fuelled partially by LPG-Diesel blends (Simulation study). Al-Qadisiyah Journal for Engineering Sciences, 15(3): 157-164. https://doi.org/10.30772/qjes.v15i3.828
[33] Kuleshov, A.S. (2006). Use of multi-zone DI diesel spray combustion model for simulation and optimization of performance and emissions of engines with multiple injection. SAE Technical Papers. https://doi.org/10.4271/2006-01-1385
[34] Rajak, U., Verma, T.N. (2018). *Spirulina* microalgae biodiesel – A novel renewable alternative energy source for compression ignition engine. Journal of Cleaner Production, 201: 343-357. https://doi.org/10.1016/j.jclepro.2018.08.057
[35] Dasari, S.R., Chaudhary, A.J., Goud, V.V., Sahoo, N., Kulkarni, V.N. (2017). In-situ alkaline transesterification of castor seeds: Optimization and engine performance, combustion and emission characteristics of blends. Energy Conversion and Management, 142: 200-214. https://doi.org/10.1016/j.enconman.2017.03.044
[36] Prakash, T., Geo, V.E., Martin, L.J., Nagalingam, B. (2018). Effect of ternary blends of bio-ethanol, diesel and castor oil on performance, emission and combustion in a CI engine. Renewable Energy, 122: 301-309. https://doi.org/10.1016/j.renene.2018.01.070
[37] Barik, D., Sivalingam, M. (2013). Performance and emission characteristics of a biogas fueled di diesel engine. SAE Technical Papers. https://doi.org/10.4271/2013-01-2507
[38] Feroskhan, M., Ismail, S., Kumar, A., Kumar, V., Aftab, S.K. (2017). Investigation of the effects of biogas flow rate and cerium oxide addition on the performance of a dual fuel CI engine. Biofuels, 8(2): 197-205. https://doi.org/10.1080/17597269.2016.1215072
[39] Verma, S., Das, L.M., Bhatti, S.S., Kaushik, S.C. (2017). A comparative exergetic performance and emission analysis of pilot diesel dual-fuel engine with biogas, CNG and hydrogen as main fuels. Energy Conversion and Management, 151: 764-777. https://doi.org/10.1016/j.enconman.2017.09.035
[40] Gürbüz, H. (2017). Experimental evaluation of combustion parameters with ion-current sensor integrated to fast response thermocouple in SI engine. Journal of Energy Engineering, 143(2): 04016046. https://doi.org/10.1061/(ASCE)EY.1943-7897.0000401
[41] Feroskhan, M., Ismail, S., Natarajan, G., Manavalla, S., Khan, T.M.Y., Khadar, S.D.A., Ali, M.A. (2023). A comprehensive study of the effects of various operating parameters on a biogas-diesel dual fuel engine. Sustainability, 15(2): 1232. https://doi.org/10.3390/su15021232
[42] Wan Osman, W.N.A., Rosli, M.H., Mazli, W.N.A., Samsuri, S. (2024). Comparative review of biodiesel production and purification. Carbon Capture Science & Technology, 13: 100264. https://doi.org/10.1016/j.ccst.2024.100264
[43] Jeswani, H.K., Chilvers, A., Azapagic, A. (2020). Environmental sustainability of biofuels: A review. Proceedings of the Royal Society A: Mathematical, Physical and Engineering Sciences, 476(2243): 20200351. https://doi.org/10.1098/rspa.2020.0351
[44] Zandie, M., Ng, H.K., Gan, S., Said, M.F.M., Cheng, X. (2022). The viability of using gasoline-integrated biodiesel–diesel mixtures in engines as a solution to greenhouse gas emissions: A review. Clean Energy, 6(6): 848-868. https://doi.org/10.1093/ce/zkac056
[45] Gürbüz, H., Köse, Ş. (2021). A theoretical investigation on the performance and combustion parameters in an spark ignition engine fueled with different shale gas mixtures. Journal of Engineering for Gas Turbines and Power, 143(6): 061015. https://doi.org/10.1115/1.4048641
[46] Enweremadu, C.C., Rutto, H.L. (2010). Combustion, emission and engine performance characteristics of used cooking oil biodiesel—A review. Renewable and Sustainable Energy Reviews, 14(9): 2863-2873. https://doi.org/10.1016/j.rser.2010.07.036
[47] Miron, L., Chiriac, R., Brabec, M., Bădescu, V. (2021). Ignition delay and its influence on the performance of a Diesel engine operating with different Diesel–biodiesel fuels. Energy Reports, 7: 5483-5494. https://doi.org/10.1016/j.egyr.2021.08.123
[48] Abishek, M.S., Kachhap, S., Rajak, U., Verma, T.N., Giri, N.C., AboRas, K.M., Elrashidi, A. (2024). Exergy-energy, sustainability, and emissions assessment of Guizotia *abyssinica* (L.) fuel blends with metallic nano additives. Scientific Reports, 14(1): 3537. https://doi.org/10.1038/s41598-024-53963-8
[49] Abishek, M.S., Kachhap, S., Rajak, U., Singh, T.S., Verma, T.N. (2024). Analysis and optimization of Guizotia *abyssinica* (L.) with alumina, titanium and diesel blends on DI engine combustion and emissions. Environment, Development and Sustainability, 26: 32163-32188. https://doi.org/10.1007/s10668-024-04841-w

NOMENCLATURE

A_0, A_2, A_3	Constants
A	Empirical factor

BSFC	Brake specific fuel consumption, kg/kWh
BSN	Number of Bosch smoke meter
BTDC	Before top dead center
BTE	Brake thermal efficiency, %
C	The cylinder's current soot concentration, m^3
CI	Compression ignition type
CN	Cetane number of fuels
C_{NO}	Empirical factor for NO_X emission
C_{PM}	Empirical factor for PM emission
CR	Compression ratio
DI	Direct injection
E_a	Apparent activation energy for the auto ignition process, kJ/Kmol.
EFM	Elementary fuel mass, kg
h_{wfr}	Height of the dense front of the NWF, m
h	Enthalpy, kJ/kg
IC	Internal combustion
l	The distance between the EFM and nozzle injector, m
l_m	The length of EFM penetration in front of spray till end, m
NO_X	Nitrogen oxides, ppm
NWF	Near wall flow
P	Current pressure in the cylinder, Pa
PM	Particulate matter, g/kWh
rpm	Revolution per minute, 1/min
rps	Revolution per second, 1/s
r_v	Relative evaporation in the different environmental zones, %
r_{vi}	The relative evaporation rate within different sections of the wall, %
S	The stroke of the piston, m
SE	Summary of (PM & NO_X emission), g/kWh
SI	Spark-ignition
SMD	Sauter mean diameter, micron
T	Temperature in the cylinder, K
t	Time, s
TDC	Top dead center
T_z	Zonal temperature, K
U	Specific internal energy, kJ/kg
V	The current speed of the EFM, m/s
$\mathbf{V_m}$	Velocity of the spray front, m/s
V	Specific volume, m^3/kg
X	Fraction of heat release
X_C	Substitute ratio of diesel fuel
X_0	Fraction of the fuel vapor formed during ignition delay and burnt